

Samirkumar R. Bhelave¹, A. N. Yerpude², S. J. Dhoble³

Photoluminescence study of Sr₃Al₃₂O₅₁:Eu³⁺ phosphor for Solid state lighting applications

¹Department of Physics, Gramgeeta Mahavidyalaya, Chimur, India

²Department of Physics, N. H. College, Bramhapuri, India, atulyerpude@gmail.com

³Department of Physics, R.T.M. Nagpur University, India

Sr₃Al₃₂O₅₁:Eu³⁺ phosphor prepared successfully by simple combustion method. Prepared matrix synthesized for different percentages of composition for rare earth Eu³⁺ = (0.5, 1.0, 1.5, 2.0, and 2.5). Photoluminescence property was taken for the given doped phosphor which shows the excitation peak at 395 nm and 466 nm respectively. Emission peaks were observed at 593 nm and 613 nm for excitation wavelength 395 nm and the same emission peak observed for excitation wavelength 466 nm was comparatively less intense than 395 nm. The phase of the synthesized phosphor confirmed by X-ray diffraction spectroscopy (XRD), Scanning electron microscopy (SEM), and Photoluminescence (PL) property shows that the given matrix is one of the potential materials that can be used for solid-state lightening.

Keywords: lanthanide; strontium aluminate phosphors; Simple combustion method; solid state lightening.

Received 08 May 2023; Accepted 13 September 2023.

Introduction

In recent days, strontium-based aluminate phosphor has attracted attraction due to its luminescence properties such as high quantum efficiency, long persistence of phosphorescence, and good stability [1–3]. In recent days inorganic light-emitting diodes (LEDs) have been widely used for different purposes due to their advantage over conventional sources [4–8]. The various rare earth (RE) elements are used for the luminescence properties in lasers, biosensors, fiber amplifiers, displays, optical thermometry, anti-counterfeiting applications, etc. [9–14]. According to the requirement of the color of emission, among them, the Eu³⁺ ion has been widely used in doping of host materials significantly for red photoluminescence due to the down-conversion process. Down conversion is an optical process in which a high-energy photon is converted into a low-energy photon [15]. According to energy level, the respective peak observed by Eu³⁺ ion due to the Charge transfer band $O^2 - Eu^{3+}$, ${}^5D_{15/2} \rightarrow {}^5L_6$, ${}^5D_{15/2} \rightarrow {}^5D_2$ respectively [16]. There are various strontium aluminate-based phosphors reported earlier such as

Sr₃La(AlO)₃(BO₃)₄ [17], SrAl₁₂O₁₉ [18], SrAl₄O₇ [19], and Sr₄Al₁₄O₂₅ [20]. In this research work the novel phosphor matrix Sr₃Al₃₂O₅₁:Eu³⁺ was synthesized and studied its photoluminescence property.

The material is subjected to structural characterizations such as X-ray diffraction (XRD), and the morphology of the given sample is determined by Scanning electron microscopy (SEM). The luminescent properties are evaluated using photoluminescence (PL) measurements in detail. The excitation spectrum shows peak positions at 257 nm, 395 nm, and 465 nm respectively for the given phosphor and emission spectra 593 nm and 613 nm respectively. The CIE diagram plotted by the color calculator of the given phosphor sample shows coordinates shifted in the red region. The given phosphor is used for red LEDs, display devices, photonic devices, and solid state lighting LEDs.

I. Experimental

The given phosphor Sr₃Al₃₂O₅₁:Eu³⁺ is prepared by simple combustion technique for various concentrations

$x = 0.5, 1.0, 1.5, 2.0,$ and 2.5 . The starting raw material required for this technique is nitrate from Strontium nitrate, Aluminum nitrate, Europium oxide, and urea used as fuel. All these ingredients were weighed properly according to stoichiometric ratio for different concentrations and mixed in an aged mortar pestle. After mixing this ingredient pesty type solution form and convert this solution into the china disk and keep it at 525°C to 550°C . First of all, the solution is boiled and dehydrated, then a decomposition process occurs with the release of large quantities of gases (oxides of carbon, nitrogen and ammonia). Within 10 to 15 minutes white aluminous powder was formed. This powder sample was allowed to cool down to room temperature, then crushed (5-10 minutes), purified the impurities sample, and then annealed at 800°C for fifteen hours [21]. A schematic representation of the combustion method for the synthesis of $\text{Sr}_3\text{Al}_{32}\text{O}_{51}:\text{Eu}^{3+}$ phosphor is shown in Fig 1. Using a Rigaku miniflex d 600 X-ray diffractometer (XRD analysis), the phase and purity of the pure sample were studied. Morphology was studied by Scanning electron microscopy (SEM) analysis using the Carl Zeiss EVO-18.

The Photoluminescence (PL) properties were examined using a SHIMADZU Spectrofluorophotometer RF-5301 PC.

II. Results and discussion

2.1. X-ray diffraction (XRD) and Scanning Electron Microscopy (SEM) analysis

Fig.2 represents the XRD analysis of the given matrix in pure form which confirms that the given phosphor matches with standard JCPDS database file no. 440024 which confirms that the given matrix prepared successfully forms a hexagonal structure. The maximum intense peak obtained at $2\theta = 33.307^{\circ}$ due to the (1 0 7) plane. Fig. 3 shows a scanning electron microscopy (SEM) micrograph of pure $\text{Sr}_3\text{Al}_{32}\text{O}_{51}$ phosphor synthesized by a simple combustion method. The SEM micrograph reveals the asymmetrical size grain type particles.

Phosphorus particles are sub-micron in size and look like agglomerates. A large

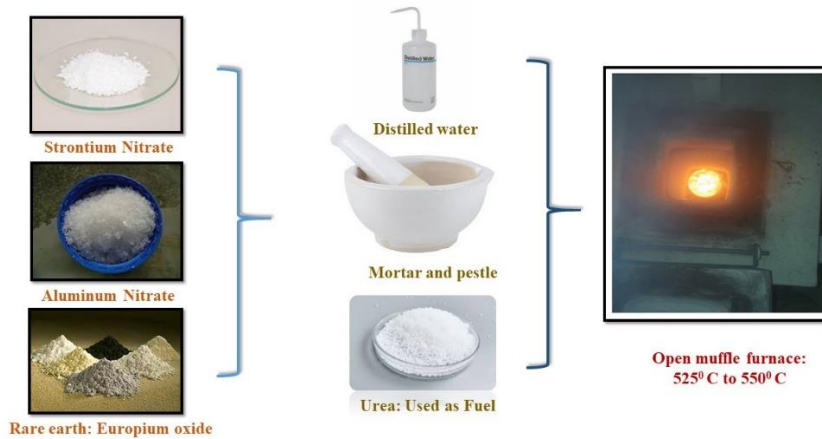


Fig. 1. Schematic representation of combustion method for the synthesis of phosphor $\text{Sr}_3\text{Al}_{32}\text{O}_{51}:\text{Eu}^{3+}$.

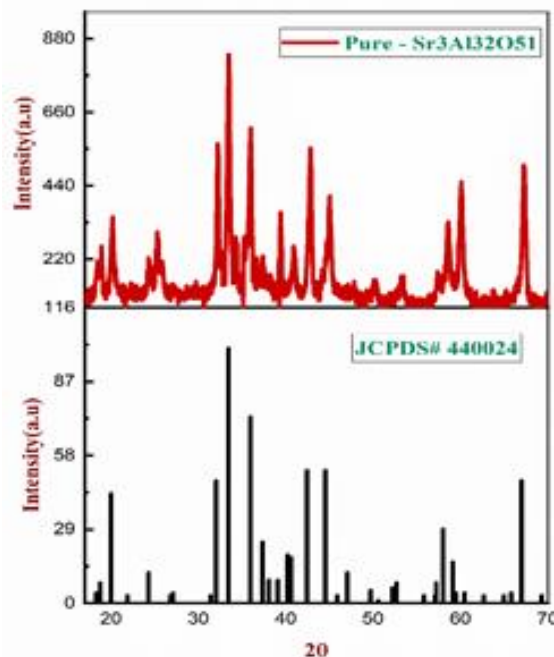


Fig. 2. XRD Analysis of the $\text{Sr}_3\text{Al}_{32}\text{O}_{51}$ pure matrix.

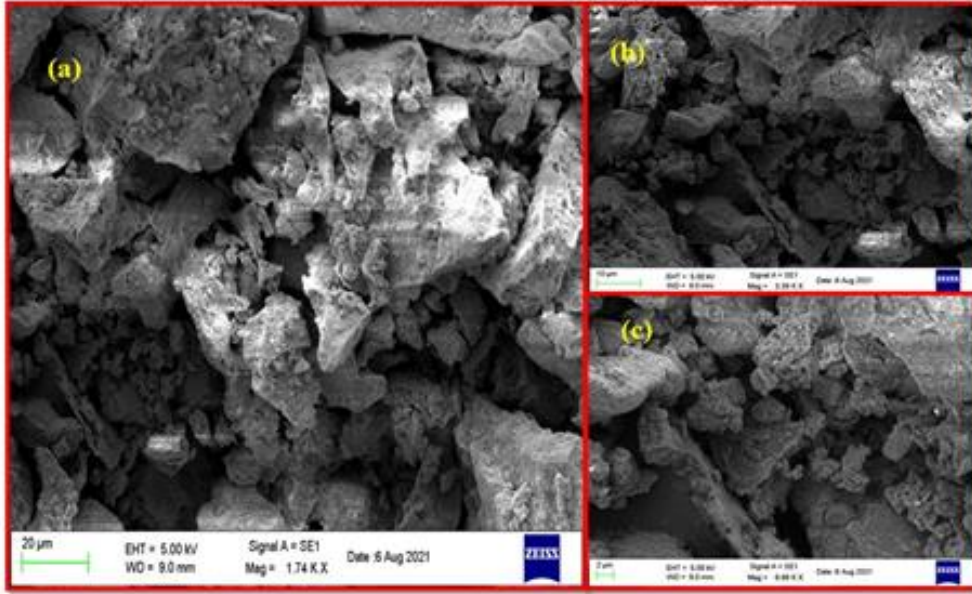


Fig. 3(a, b, c). SEM micrograph of $\text{Sr}_3\text{Al}_32\text{O}_{51}$ phosphor at different magnification 20 μm , 10 μm and 2 μm .

amount of gases is released in an exothermic combustion reaction. Although the particles are near to each other due to the necking which shows a spherical surface while size is in micrometer. The morphology shown in Fig. 3 reveals that the given phosphor be one of a useful candidate for solid-state lighting [22-23].

2.2. Photoluminescence (PL) study

Fig. 4 represents the energy level diagram of the Eu^{3+} ion. The energy level diagram is the important one to understand the phenomenon of photoluminescence, as shown in Fig. 4 the two important emission peaks obtained generally in the Eu^{3+} ion due to the transition between the $^5\text{D}_0 \rightarrow ^7\text{F}_1$, $^5\text{D}_0 \rightarrow ^5\text{F}_2$ [24]. The excitation spectrum as shown in Fig. 5 of $\text{Sr}_3\text{Al}_32\text{O}_{51}:\text{Eu}^{3+}$ shows the peak position at 257 nm, 395 nm and 465 nm. According to the energy level diagram the respective excitation peaks observed by the Charge transfer band $\text{O}^{2-} - \text{Eu}^{3+}$, $^5\text{D}_{15/2} \rightarrow ^5\text{L}_6$, $^5\text{D}_{15/2} \rightarrow ^5\text{D}_2$ respectively [25]. Here important charge transfer band is obtained for the given phosphor which is used in the energy transfer process. Fig. 6 (a, b, c) shows the Photoluminescence (PL) emission spectrum of Eu^{3+} ion-activated phosphor $\text{Sr}_3\text{Al}_32\text{O}_{51}:\text{Eu}^{3+}$ at excitation wavelengths of $\lambda_{\text{ex}} = 257$ nm, 465 nm and 395 nm. The emission spectra show intense peak positions at 593 nm and 613 nm respectively [26]. The peak pattern is the same for all the concentrations while intensity may vary with the increase of concentration. On increasing the concentration ($x = 0.5$ to 2.5 mole %) intensity increases up to 2.0 mole% and above that intensity declines means the concentration quenching occurs at 2.0 mole% for the given phosphor. Concentration quenching effect observed at all excitation wavelengths $\lambda_{\text{ex}} = 257$ nm, 395 nm, and 465 nm at 2.0 mole%. The concentration quenching mainly occurs due to the critical transfer distance [27,28]. On comparing luminescence emission intensity most intense peak was obtained for $\lambda_{\text{ex}} = 257$ nm as shown in Fig. 6 (d).

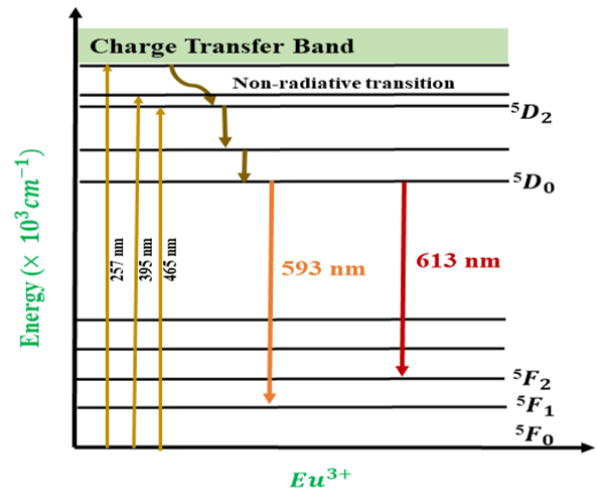


Fig. 4. Energy level diagram: Eu^{3+} ion.

2.3. CIE Chromaticity

The CIE chromaticity of the $\text{Sr}_3\text{Al}_32\text{O}_{51}:\text{Eu}^{3+}$ phosphor spectrum excited by 257 nm light using the CIE 1931 color matching function as shown in Fig. 7. Chromaticity diagram of $\text{Sr}_3\text{Al}_32\text{O}_{51}:\text{Eu}^{3+}$ phosphor intimates the CIE coordinates for $\text{Sr}_3\text{Al}_32\text{O}_{51}:\text{Eu}^{3+}$ phosphor to be at (0.5074, 0.4876) in the red region. To study the variation of PL intensity with the concentration of Eu^{3+} ion in the host $\text{Sr}_3\text{Al}_32\text{O}_5$, a series of samples ($x = 0.5, 1.0, 1.5, 2.0, 2.5$ mole %) were synthesized. The red emission intensity increased with the increase in Eu^{3+} ion concentration and the maximum intensity was obtained for 2.0 mole %. The color purity of the synthesized phosphor was determined by using the formula [29,30]:

$$\text{Color purity} = \frac{\sqrt{(x-x_i)^2 + (y-y_i)^2}}{\sqrt{(x_d-x_i)^2 + (y_d-y_i)^2}} * 100 \%$$

Where, (x, y) and (xi, yi) are the color coordinates of the sample point and the CIE equal-energy illuminant,

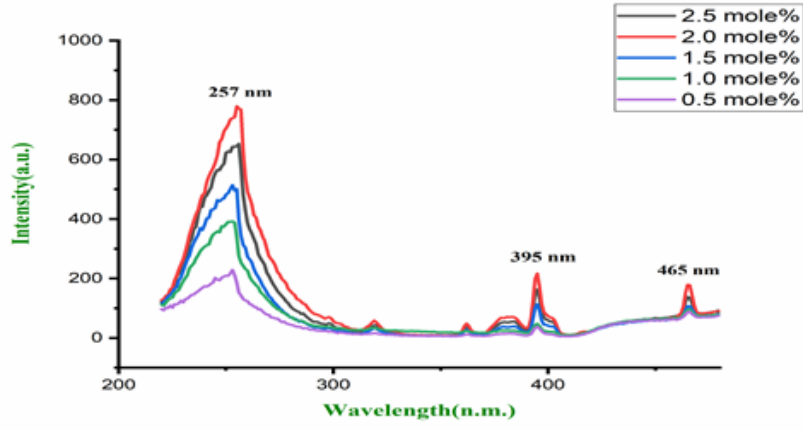


Fig. 5. shows the Photoluminescence (PI) excitation spectra for the Sr₃Al₃₂O₅₁:Eu³⁺.

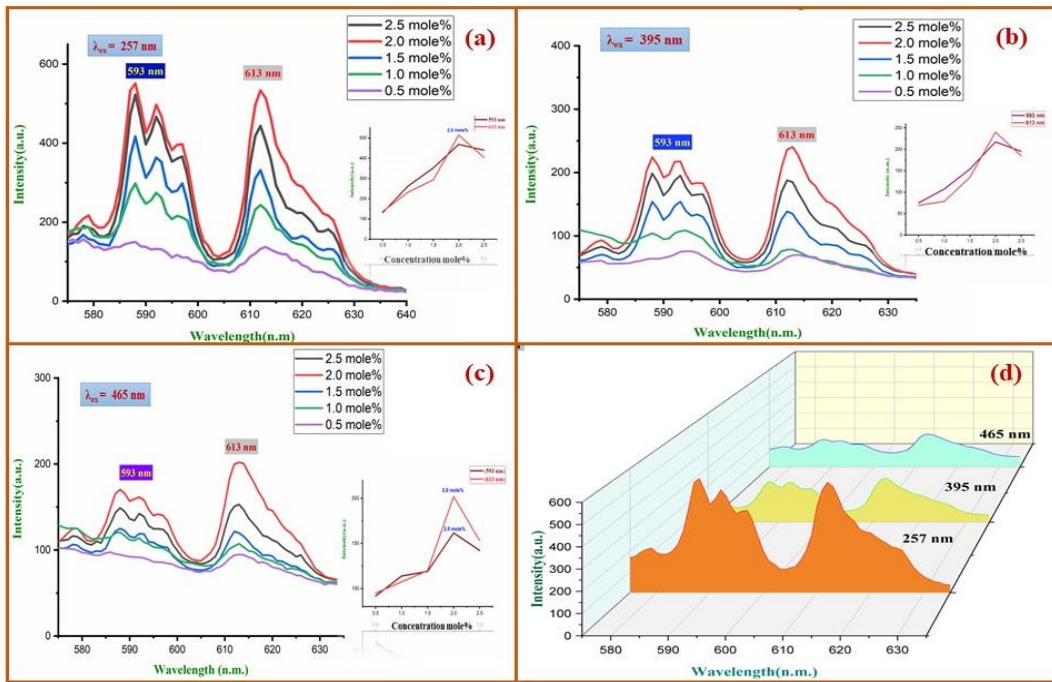


Fig. 6. Emission spectra of Sr₃Al₃₂O₅₁:Eu³⁺ phosphor at (a) $\lambda_{ex} = 257$ nm (b) $\lambda_{ex} = 395$ nm (c) $\lambda_{ex} = 465$ nm (d) Comparison of emission spectra at $\lambda_{ex} = 257$ nm, $\lambda_{ex} = 395$ nm and $\lambda_{ex} = 465$ nm.

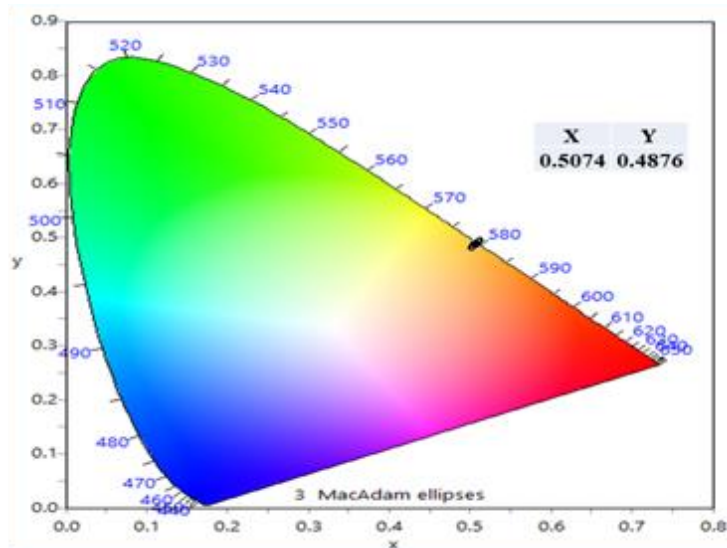


Fig.7. CIE chromaticity diagram using a 1931 color calculator function.

respectively; (xd, yd) is the chromaticity coordinate of the dominant wavelength of the light source. For $\text{Sr}_3\text{Al}_3\text{O}_{51}:\text{Eu}^{3+}$ 2.0 mole % sample, the co-ordinates of (x, y) are (0.5074, 0.4876); coordinates of (xi, yi) are (0.333, 0.333); and dominant coordinates (xd, yd) are calculated taking values corresponding to dominant wavelength 257 nm which is (0.6722, 0.3276), substituting these values in above equation color purity of $\text{Sr}_3\text{Al}_3\text{O}_{51}:\text{Eu}^{3+}$ at 2.0 mole % sample was found to be 58.45 %. Therefore, the present $\text{Sr}_3\text{Al}_3\text{O}_{51}:\text{Eu}^{3+}$ sample showed good color purity and can be a potential red-emitting phosphor. The diagram shows that the given phosphor should be a potential candidate for red light emission.

Conclusion

$\text{Sr}_3\text{Al}_3\text{O}_{51}:\text{Eu}^{3+}$ phosphors were successfully synthesized by a simple combustion method where urea used as a fuel. XRD analysis data shown prepared sample is properly matched with standard JCPDS data file no.

440024 confirms the phase purity of the given matrix. All diffraction peaks were indexed with standard data of $\text{Sr}_3\text{Al}_3\text{O}_{51}$ phosphor means XRD Analysis confirms that given phosphor was synthesized successfully. Matrix $\text{Sr}_3\text{Al}_3\text{O}_{51}:\text{Eu}^{3+}$ gives proper peak position for Eu^{3+} ion at 593 nm and 613 nm. Concentration quenching occurs at 2.0 mole%. The morphology of a given phosphor is studied by SEM micrograph analysis which conforms to the particle size in a micrometer. All these studies shows that the novel matrix $\text{Sr}_3\text{Al}_3\text{O}_{51}:\text{Eu}^{3+}$ is one of the useful potential phosphors for red LEDs and solid-state lightening application.

Bhelave Samirkumar R. – Assistant Professor
Department of Physics;
Yerpude A. N. – Ph.D, MSc(Physics) Department of Physics;
Dhoble S. J. –, Ph.D. MSc (Physics) Department of Physics.

- [1] Y. Ma, S. Chen, J. Che, J. Wang, R. Kang, J Zhao, B. Deng, R. Yu, H. Geng, *Effect of charge compensators (Li^+ , Na^+ , K^+) on the luminescence properties of $\text{Sr}_3\text{TeO}_6:\text{Eu}^{3+}$ red phosphor*, Journal Ceramics International, 47(6), 8518 (2021); <https://doi.org/10.1016/j.ceramint.2020.11.219>.
- [2] S.R. Bhelave, A.N. Yerpude, S.J. Dhoble, *Comparative photoluminescence study of $\text{MAIB}_3\text{O}_7:\text{Dy}^{3+}$ ($M=\text{Ca}, \text{Sr}$) phosphor for solid-state lighting applications*, Journal of Optics, (2023); <https://doi.org/10.1007/s12596-023-01259-x>.
- [3] S R Bhelave, A N Yerpude, V R Panse, A Saregar, S J Dhoble, *Study the photoluminescence properties of $\text{Ca}_4\text{Al}_4\text{O}_{25}:\text{Dy}^{3+}$ phosphor for solid state lighting*, AIP Conference Proceedings 2595(1), 030003 (2023); <https://doi.org/10.1063/5.0123776>.
- [4] V R Panse, S R Bhelave, A N Yerpude, A Saregar, S J Dhoble, *Photoluminescence properties of $\text{Ca}_2\text{Al}_2\text{O}_5:\text{Sm}^{3+}$ down conversion phosphor for eco-friendly solid state lighting applications*, AIP Conference, Proceedings 2595(1), 030008 (2023); <https://doi.org/10.1063/5.0123777>.
- [5] L Zhou, P Du, L Li, *Facile modulation the sensitivity of $\text{Eu}^{2+}/\text{Eu}^{3+}$ -coactivated $\text{Li}_2\text{CaSiO}_4$ phosphors through adjusting spatial mode and doping concentration*, Scientific report, 20180 (2020); <https://doi.org/10.1038/s41598-020-77185-w>.
- [6] Z Ming, J Qiao, M S Molokeev, J. Zhao, H C Swart, Z Xia, *Multiple Substitution Strategies toward Tunable Luminescence in $\text{Lu}_2\text{MgAl}_4\text{SiO}_{12}:\text{Eu}^{2+}$ Phosphors*, American Chemical Society, 59(2), 1405 (2020); <https://doi.org/10.1021/acs.inorgchem.9b03142>.
- [7] R Yantake, A Sidike, T Yusufu, *Effect of Eu^{3+} doping on luminescence properties of a $\text{KAlSiO}_4:\text{Sm}^{3+}$ phosphor*, Journal of Rare Earths, 40(3), 390 (2022); <https://doi.org/10.1016/j.jre.2020.10.022>.
- [8] V Havasi, D Tátrai, G Szabó, et al, *On the effects of milling and thermal regeneration on the luminescence properties of Eu^{2+} and Dy^{3+} doped strontium aluminate phosphors*, Journal of Luminescence, 219, 116917 (2020); <https://doi.org/10.1016/j.jlumin.2019.116917>.
- [9] C Li, B Zheng, Y Liu, et al., *A boosting upconversion luminescent resonance energy transfer and biomimetic periodic chip integrated CRISPR/Cas12a biosensor for functional DNA regulated transduction of non-nucleic acid targets*, Biosensors and Bioelectronics, 169, 112650 (2020); <https://doi.org/10.1016/j.bios.2020.112650>.
- [10] J Xu, S Tanabe, *Persistent luminescence instead of phosphorescence: History, mechanism, and perspective*, Journal of Luminescence, 205, 581 (2018); <https://doi.org/10.1016/j.jlumin.2018.09.047>.
- [11] M Back, E Casagrande, C A Brondin, M Back, E Casagrande, C A Brondin, E Ambrosi, D Cristofori, J Ueda, S Tanabe, E Trave, P. Riello, *Lanthanide-Doped $\text{Bi}_2\text{SiO}_5@ \text{SiO}_2$ Core-Shell Upconverting Nanoparticles for Stable Ratiometric Optical Thermometry*, ACS Applied Nano Materials, 3(3), 2594 (2020); <https://doi.org/10.1021/acsnm.0c00003>.
- [12] Yu Ding, Ning Guo, Xiang Lü, Huitao Zhou, Lu Wang, Ruizhuo Ouyang, Yuqing Miao, Baiqi Sha, *None-rare-earth activated $\text{Ca}_{14}\text{Al}_{10}\text{Zn}_6\text{O}_{35}:\text{Bi}^{3+}, \text{Mn}^{4+}$ phosphor involving dual luminescent centers for temperature sensing*, The American Ceramic Society, (2019); <https://doi.org/10.1111/jace.16660>.
- [13] M Li, W Yao, J Liu, et al., *Facile synthesis and screen printing of dual-mode luminescent $\text{NaYF}_4:\text{Er}, \text{Yb}$ (Tm)/carbon dots for anti-counterfeiting applications*, Journal of Materials Chemistr C, 5, 6512 (2017); <https://doi.org/10.1039/c7tc01585b>.

- [14] A R Kadam, R S Yadav, G C Mishra, S J Dhoble, *Effect of singly, doubly and triply ionized ions on downconversion photoluminescence in Eu^{3+} doped $\text{Na}_2\text{Sr}_2\text{Al}_2\text{PO}_4\text{Cl}_9$ phosphor: A comparative study*, *Ceramics International*, 46(3), 3264 (2020); <https://doi.org/10.1016/j.ceramint.2019.10.032>.
- [15] S R Bhelave, A R Kadam, A N Yerpude, S J Dhoble, *Intensity enhancement of photoluminescence in $\text{Tb}^{3+}/\text{Eu}^{3+}$ co-doped $\text{Ca}_{14}\text{Zn}_6\text{Al}_{10}\text{O}_{35}$ phosphor for WLEDs*, *Luminescence*, 1 (2023); <https://doi.org/10.1002/bio.4456>.
- [16] R E Rojas-Hernandez, F Rubio-Marcos, M Á Rodríguez, F Fernandez, *Long lasting phosphors: $\text{SrAl}_2\text{O}_4:\text{Eu}$, Dy as the most studied material*, *Renewable and Sustainable Energy Reviews* 81, 2759 (2018); <https://doi.org/10.1016/j.rser.2017.06.081>.
- [17] A M Srivastava, W W Beersb, *Luminescence of Pr^{3+} in $\text{SrAl}_{12}\text{O}_{19}$: Observation of two photon luminescence in oxide lattice*, *Journal of Luminescence*, 71(4), 285 (1997); [https://doi.org/10.1016/S0022-2313\(96\)00221-9](https://doi.org/10.1016/S0022-2313(96)00221-9).
- [18] T Sasaki, J Fukushima, Y Hayashi, H Takizawa, *Synthesis and photoluminescence properties of a novel $\text{Sr}_2\text{Al}_6\text{O}_{11}:\text{Mn}^{4+}$ red phosphor prepared with a B_2O_3 flux*, *Journal of Luminescence* 194, 446 (2018); <https://doi.org/10.1016/j.jlumin.2017.10.076>.
- [19] H Liu, X Liu, X Wang, et al., *Unusual concentration induced antithermal quenching of the Eu^{2+} emission at 490 nm in $\text{Sr}_4\text{Al}_{14}\text{O}_{25}:\text{Eu}^{2+}$ for near ultraviolet excited white LEDs*, *Journal of the American Ceramic Society* 103, 5758 (2020); <https://doi.org/10.1111/jace.17306>.
- [20] Y R Parauha, V Sahu, S J Dhoble, *Prospective of combustion method for preparation of nanomaterials: A challenge*, *Solid-State Materials for Advanced Technology*, 267(2), 115054 (2021); <https://doi.org/10.1016/j.mseb.2021.115054>.
- [21] A R Kadam, S J Dhoble, *Synthesis and luminescence study of Eu^{3+} -doped SrYAl_3O_7 phosphor*, *Luminescence*, 34(8), 1 (2019); <https://doi.org/10.1002/bio.3681>.
- [22] A R Kadam, G C Mishra, A D Deshmukh, S J Dhoble, *Enhancement of blue emission in Ce^{3+} , Eu^{2+} activated BaSiF_6 downconversion phosphor by energy transfer mechanism: a photochromic phosphor*, *Journal of Luminescence* 229, 117676 (2021); <https://doi.org/10.1016/j.jlumin.2020.117676>.
- [23] Y Wang, Y Ke, S Chen, et al., *Luminescence investigation of red-emitting $\text{Sr}_2\text{MgMoO}_6:\text{Eu}^{3+}$ phosphor for visualization of latent fingerprint*, *Journal of Colloid And Interface Science* 583, 89 (2021); <https://doi.org/10.1016/j.jcis.2020.09.024>.
- [24] M T Tran, N Tu, N V Quang, et al., *Excellent thermal stability and high quantum efficiency orange-red-emitting $\text{AlPO}_4:\text{Eu}^{3+}$ phosphors for WLED application*, *Journal of Alloys and Compounds* 853, 156941 (2021); <https://doi.org/10.1016/j.jallcom.2020.156941>.
- [25] S K Ramteke, A N Yerpude, S J Dhoble, N S Kokode, *Luminescence characterization of $\text{KBaPO}_4:\text{RE}$ ($\text{RE} = \text{Sm}^{3+}, \text{Eu}^{3+}, \text{Dy}^{3+}$) phosphors*, *Luminescence*, 969 (2020); <https://doi.org/10.1002/bio.3792>.
- [26] Q Liu, F Meng, X Zhang, et al., *Al^{3+} -doping-induced enhancement of $\text{Tb}_3\text{Ga}_5\text{O}_{12}:\text{Eu}^{3+}$ orange light-emitting phosphor photoluminescence for white light-emitting diodes*, *Journal of Luminescence* 226, 117505 (2020); <https://doi.org/10.1016/j.jlumin.2020.117505>.
- [27] W Hami, D Zambon, A Zegzouti, et al., *Application of spectroscopic properties of Eu^{3+} ion to predict the site symmetry of active ions in $\text{AgLaP}_2\text{O}_7:\text{Eu}^{3+}$ phosphors*, *Inorganic Chemistry Communications* 107, 107475 (2019); <https://doi.org/10.1016/j.inoche.2019.107475>.
- [28] A Kumar, S J Dhoble, J Bhatt, et al., *Structural characterization and influence of calcination temperature on luminescence properties of $\text{Sr}_{0.91}\text{Mg}_2\text{Al}_{5.82}\text{Si}_{9.18}\text{O}_{30}:\text{Eu}^{3+}$ nanophosphors*, *Powder Technology* 354, 591 (2019); <https://doi.org/10.1016/j.powtec.2019.06.031>.
- [29] M Pokhrel, G A Kumar, C Ma, M G Brik, B W Langloss, I. N Stanton, J Michael, D K Sardar, Y Mao, *Electronic and optical properties of Er-doped Y_2O_3 phosphors*, *Materials Chemistry C.*, 3, 11486 (2015); <https://doi.org/10.1039/C5TC02665B>.
- [30] J Xiang, M Yang, Y Che, J Zhu, Y Mao, K Xiong, H Zhao, *Photoluminescence investigation of novel reddish-orange phosphor $\text{Li}_2\text{NaBP}_2\text{O}_8:\text{Sm}^{3+}$ with high CP and low CCT*, *Ceramics International* 45, 7018 (2019); <https://doi.org/10.1016/j.ceramint.2018.12.203>.

С. Р. Бхелаве¹, А. Н. Єрпуде², С. Дж. Добле³

Дослідження фотолюмінесценції люмінофора $\text{Sr}_3\text{Al}_3\text{O}_{51}:\text{Eu}^{3+}$ для твердотілого освітлення

¹Кафедра фізики, Грамгіта Махавідьялая, Чимур, Індія

²Кафедра фізики, Н. Х. коледж, Брамханури, Індія, atulyerpude@gmail.com

³Кафедра фізики Р.Т.М. університет Нагпуру, Індія

Люмінофор $\text{Sr}_3\text{Al}_3\text{O}_{51}:\text{Eu}^{3+}$ отримано методом простого спалювання. Підготовлена матриця, синтезована для різних відсотків складу рідкоземельного Eu^{3+} = (0,5; 1,0; 1,5; 2,0 і 2,5). Властивість фотолюмінесценції взято для даного легованого люмінофора, який демонструє пік збудження при 395 нм і 466 нм. Піки випромінювання спостерігалися при 593 нм і 613 нм для довжини хвилі збудження 395 нм, і той самий пік випромінювання, що спостерігався для довжини хвилі збудження 466 нм був порівняно менш інтенсивним, ніж 395 нм. Фаза синтезованого люмінофора, яка підтверджена рентгенівською дифракційною спектроскопією (XRD), скануючою електронною мікроскопією (SEM) і властивістю фотолюмінесценції (PL), показує, що дана матриця є одним із потенційних матеріалів, які можуть бути використані для твердотілого освітлення.

Ключові слова: лантаноїди; люмінофори алюмінату стронцію; спосіб простого спалювання; твердотіле освітлення.